Journal of Inorganic Biochemistry 247 (2023) 112331

Contents lists available at ScienceDirect

Journal of Inorganic Biochemistry

journal homepage: www.elsevier.com/locate/jinorgbio

Organomercury oligonucleotide conjugates as artificial ribonucleases

Lange Yakubu Saleh, Mikko Ora, Tuomas Lönnberg *

Department of Chemistry, University of Turku, Henrikinkatu 2, 20500 Turku, Finland

ARTICLE INFO

Keywords:
RNA
Hydrolysis
Organometallic
Mercury
Catalysis
Oligonucleotide

ABSTRACT

Two oligonucleotide conjugates sharing the same sequence but incorporating a different 5′-terminal organometallic moiety were synthesized, by either direct mercuration in solution or oximation with an organomercury aldehyde on solid support. The potential of these conjugates to serve as new type of artificial ribonucleases was tested with a complementary 2′-*O*-methyl-RNA target sequence featuring a single cleavable RNA phosphodiester linkage. Both organomercury oligonucleotides greatly outperformed their metal-free counterparts as well as the previously reported small molecule organomercury RNA cleaving agent in catalytic activity, providing an important proof-of-concept. Compared to state-of-the-art metal-dependent artificial ribonucleases, however, the observed activity was modest.

1. Introduction

Artificial ribonucleases [1–4] are a class of synthetic molecules that have been designed to serve as restriction enzymes to selectively manipulate large RNA sequences in a laboratory setting or to target and cleave pathogenic RNA molecules *in vivo* with high precision. In either case, selectivity is achieved in a programmable manner by tethering the cleaving agent to a guiding oligonucleotide strand complementary to the target sequence. Unlike classical antisense oligonucleotides, artificial ribonucleases would not be dependent on endogenous RNase H activity for cleavage of the target mRNA, allowing more extensive modification of the guiding strand to address issues with intracellular delivery and stability [5–8]. The feasibility of this approach has been demonstrated recently [9].

The artificial ribonucleases reported so far can be categorized as either metal-free or metal-dependent. In the former, the cleaving agent is an organic moiety, such as an imidazole or guanidine cluster [10–16] or a short peptide [9,17–19]. The latter group, in turn, relies on coordinative complexes of metal ions for cleavage activity [20–25]. Metal catalysts generally exhibit higher cleavage activity than organic ones but are susceptible to dissociation under the metal-deficient physiological conditions. The most efficient Zn(II)-dependent artificial ribonucleases, however, achieve promising cleavage activity at Zn(II) concentrations approaching those found in malaria-infected red blood cells [26,27].

Organometallic complexes could, in principle, combine the catalytic efficiency of metal-dependent RNA cleaving agents with the hydrolytic stability of organic ones. We have recently reported on the first steps taken on this path, assessing the ability of the arylmercury complex 14-(2,4-dimethyl-6-mercuriphenoxy)-3,6,9,12-tetraoxatetradecan-1-ol to catalyze the hydrolysis of the RNA model compound adenylyl-3′,5′-(2′,3′-*O*-methyleneadenosine) [28]. The choice of the catalyst was motivated by easy accessibility, aqueous solubility and hydrolytic stability, rather than expected catalytic efficiency. Nevertheless, a rate acceleration of an order of magnitude was observed at neutral pH. Furthermore, dependence of the rate on catalyst concentration was linear over the entire range studied (limited by solubility of the catalyst), indicating potential for higher efficiency if the local catalyst concentration could be increased. With artificial ribonucleases, this would be achieved by tethering the catalyst to a guiding oligonucleotide sequence. This article describes the synthesis and kinetic studies of such conjugates, both with the previously employed 2,4-dimethyl-6-mercuriphenyl cleaving agent well as a new 4-hydroxy-3,5-dimercuriphenyl one.

2. Results and discussion

2.1. Building block synthesis

Preparation of phosphoramidite building block **1** is outlined in Scheme 1. Triethylene glycol was first tosylated in the presence of silver oxide and sodium iodide in dichloromethane. The tosylate group of intermediate **2** was then displaced by 2,4-dimethylphenol in DMF, with potassium carbonate as the base. Finally, the resulting alcohol **3** was phosphitylated with 2-cyanoethyl-*N*,*N*-diisopropylchlorophosphoramidite in the presence of

* Corresponding author.
E-mail address: tuanlo@utu.fi (T. Lönnberg).

https://doi.org/10.1016/j.jinorgbio.2023.112331
Received 30 May 2023; Received in revised form 3 July 2023; Accepted 12 July 2023
Available online 17 July 2023

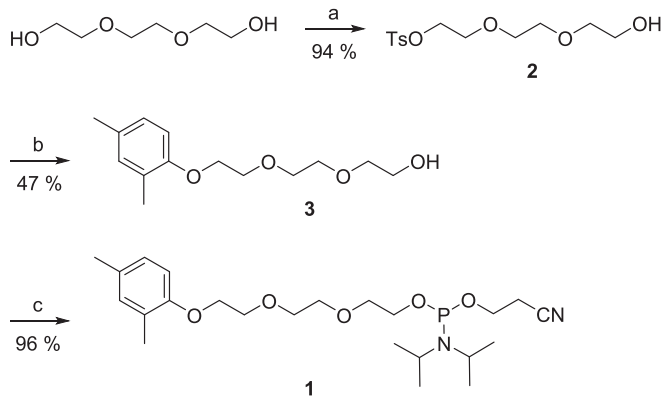

Scheme 1. Synthesis of phosphoramidite building block **1**. Reagents and conditions: a) TsCl, Ag_2O, NaI, CH_2Cl_2, 25 °C, 30 min; b) 2,4-dimethylphenol, K_2CO_3, DMF, reflux, 16 h; c) 2-cyanoethyl-*N*,*N*-diisopropylchlorophosphoramidite, Et_3N, CH_2Cl_2, N_2 atmosphere, 25 °C, 2 h.

triethylamine in dichloromethane, affording the desired building block **1**.

2.2. Oligonucleotide synthesis

Table 1 summarizes the sequences of the oligonucleotides used in the present study. All oligonucleotides were assembled by conventional phosphoramidite strategy on an automated DNA/RNA synthesizer. The target strand **ON2** was synthesized from standard commercial building blocks and incorporated a single RNA residue as the designated cleavage site, the rest of the sequence being 2′-*O*-methylated. The artificial ribonuclease oligonucleotides **ON1x** and **ON1y** were also synthesized from commercial 2′-*O*-methyl-RNA building blocks and in each case the building block generating a metalation site (either **1** or the previously reported [29,30] 2-(phthaliminooxy)ethyl-2-cyanoethyl-*N*,*N*-diisopropylphosphoramidite) was coupled at the 5′-terminus (Scheme 2). In addition, C5-methylated versions of cytidine and uridine building blocks were used in **ON1x** to prevent mercuration of this reactive site.

The phthaloyl protection of **ON1y** was removed on solid support by treatment with hydrazine hydrate in a mixture of pyridine and acetic acid. The newly exposed aminooxy function was then immediately subjected to oxime coupling with either 4-hydroxybenzaldehyde or 3,5-bis(acetoxymercuri)-4-hydroxybenzaldehyde [31], as described previously (Scheme 2B) [32]. All oligonucleotides were released from the solid support and their base and phosphate protections removed by conventional ammonolysis. In contrast to **ON1y**, **ON1x** was mercurated in solution phase by treatment with mercuric acetate, affording **ON1x-Hg** (Scheme 2A). Finally, all oligonucleotides were purified by RP-HPLC, characterized mass spectrometrically and quantified UV spectrophotometrically.

2.3. Hybridization studies

The modest activity of the previously reported [28] 14-(2,4-dimethyl-6-mercuriphenoxy)-3,6,9,12-tetraoxatetradecan-1-ol catalyst suggested that an elevated temperature might be necessary also in the present case to bring the cleavage reaction to a reasonable timescale for kinetic studies. On the other hand, very high temperatures would compromise hybridization of the artificial ribonuclease with the target sequence. To establish the highest temperature applicable, UV melting profiles (Fig. S18—S21 in the Supporting Information) of the duplexes formed by **ON1x**, **ON1x-Hg**, **ON1y** and **ON1y-Hg_2** with the target oligonucleotide **ON2** were recorded over a range of 10—90 °C at pH = 7.4 (20 mM cacodylate buffer) and I = 0.10 M (adjusted with sodium perchlorate). The melting temperatures of all duplexes were too high to determine accurately and no denaturation could be observed below 60 °C. 55 °C was, hence, deemed as a suitable temperature for the kinetic studies.

Table 1
Sequences of the oligonucleotides used in the present study.

Oligonucleotide	Sequence[a]
ON1x	5′-X c^mga $c^m c^m$g au$^m c^m$ c^mag c^mgg-3′
ON1x-Hg	5′-Hg-X c^mga $c^m c^m$g au$^m c^m$ c^mag c^mgg – 3′
ON1y	5′-Y cga ccg auc cag cgg-3′
ON1y-Hg_2	5′-Hg_2-Y cga ccg auc cag cgg-3′
ON2	5′-ccg cug gau cgg ucG aga gga gug a-3′

[a] Lowercase letters refer to 2′-*O*-methylribonucleotide and capital letters to ribonucleotide residues. "c^m" and "u^m" refer to C5-methylated versions of the respective nucleotides. For structures of the modified residues X, Hg-X, Y and Hg_2-Y, see Scheme 2.

2.4. Cleavage studies

The ability of the organomercury oligonucleotide conjugates **ON1x-Hg** and **ON1y-Hg_2** to catalyze the cleavage of the complementary target oligonucleotide **ON2** was studied at pH = 7.4 (20 mM cacodylate buffer) and T = 55 °C. To simplify the product mixture, **ON2** bore only a single ribonucleotide residue near the 5′-terminus (and thus the active site) of the cleaving agent and the rest of the sequence was 2′-*O*-methylated. The use of such chimeric oligonucleotides as model compounds was pioneered already in the 1990s [33]. For a negative control, similar mixtures were prepared also with the unmercurated analogues of the cleaving agents (**ON1x** and **ON1y**). Each reaction mixture contained a 0.20 μM concentration of both the target strand and the artificial ribonuclease (or its unmercurated counterpart). Samples withdrawn from the reaction mixtures at appropriate time intervals were analyzed by anion exchange HPLC (Fig. S22—S25 in the Supporting Information) and the identity of the products was established by RP-UPLC-MS (Fig. S26 and S27 in the Supporting Information).

With both **ON1x-Hg** and **ON1y-Hg_2** as the artificial ribonuclease, cleavage of **ON2** to the expected products, namely the upstream 15-mer oligonucleotide with a 2′,3′-cyclic monophosphate terminus and the downstream 10-mer oligonucleotide with a 5′-alcohol terminus, were observed (Scheme 3). Quantification of these products proved challenging as satisfactory chromatographic separation could not be achieved despite extensive screening of various solvent systems. The peak corresponding to the starting material **ON2**, however, could be integrated reliably so determination of reaction rates was based on its time-dependent diminution (Fig. 1).

As seen in Fig. 1, **ON2** was hardly cleaved in the presence of the unmercurated oligonucleotide **ON1x**. With the other unmercurated oligonucleotide **ON1y**, on the other hand, some cleavage could be observed. The mercurated artificial ribonucleases **ON1x-Hg** and **ON1y-Hg_2** clearly outperformed their unmercurated counterparts, **ON1x-Hg** being more efficient of the two. In both cases, some **ON2a** appeared to remain at equilibrium but we argue that this is due to peaks of **ON2a** and the artificial ribonuclease overlapping, rather than the reaction slowing down. Indeed, UPLC-MS analysis revealed both **ON1x-Hg** and **ON1y-Hg_2** to be mostly intact at the end of the kinetic runs (data not shown).

First-order rate constants for the cleavage of **ON2** were obtained by non-linear least-squares fitting of the experimental data presented in Fig. 1 to Eq. (1).

$$c_t = (c_0 - c_{eq})(1 - e^{-k_{obs}t}) + c_{eq} \quad (1)$$

c_t, c_0 and c_{eq} are relative concentrations of **ON2** at time point t, in the beginning of the kinetic run and at equilibrium, respectively. k_{obs} is the first-order rate constant and t the sampling time. The results of the fitting are summarized in Table 2.

Comparison of the rate constant of **ON1x-Hg**-catalyzed cleavage of **ON2** with the one previously reported for the cleavage of a dinucleotide model compound catalyzed by a related small molecule cleaving agent

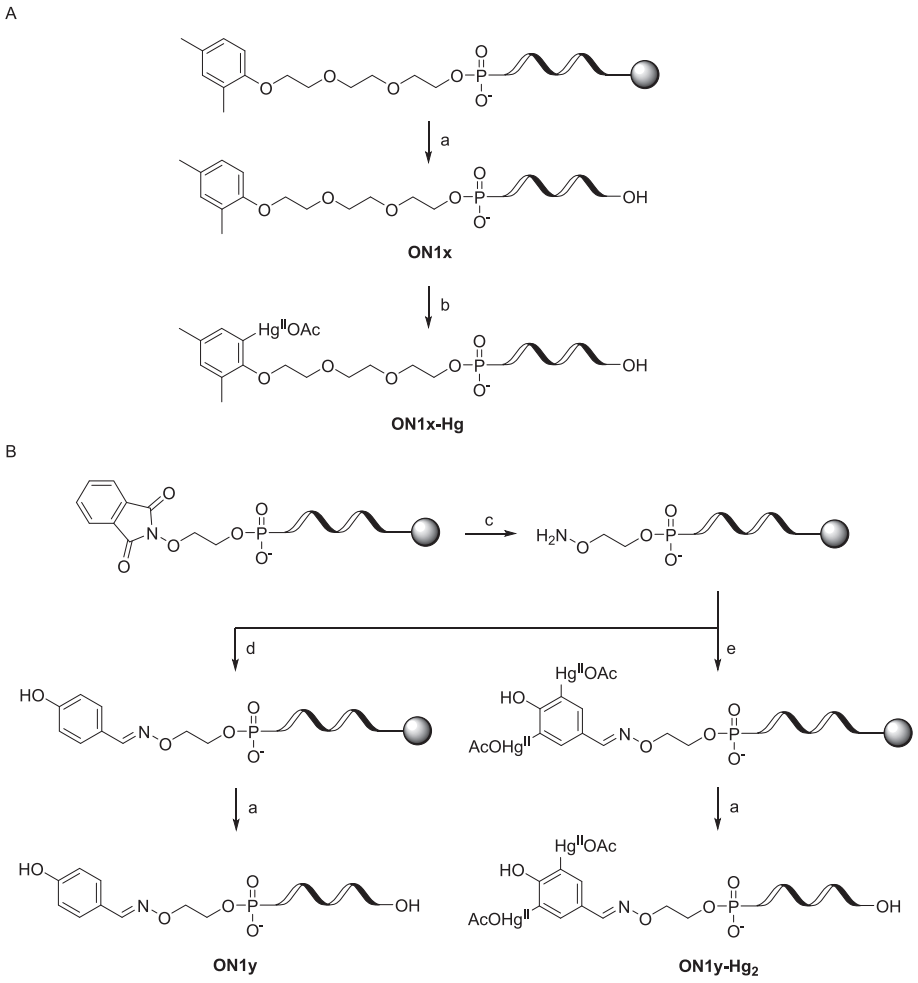

Scheme 2. Synthesis of oligonucleotide conjugates A) **ON1x** and **ON1x-Hg** and B) **ON1y** and **ON1y-Hg$_2$**. Reagents and conditions: a) NH_3, H_2O, 25 °C, 16 h; b) $Hg(OAc)_2$, H_2O, 55 °C, 22 h; c) H_2NNH_2, H_2O, AcOH, pyridine, 25 °C, 45 min; d) 4-hydroxybenzaldehyde, pyridine, 25 °C, 2 h; e) 3,5-bis(acetoxymercury)-4-hydroxybenzaldehyde, pyridine, 25 °C, 2 h.

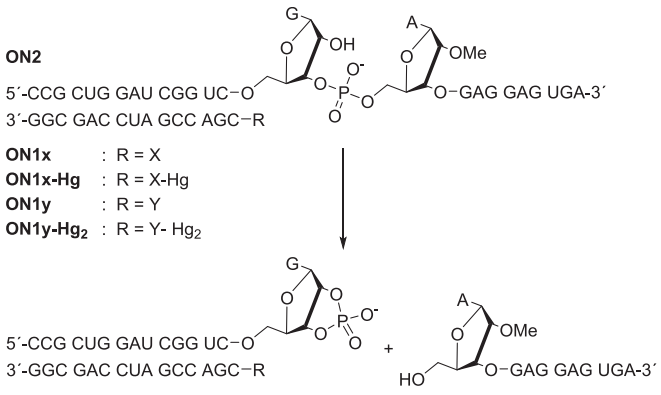

Scheme 3. Cleavage of the target oligonucleotide **ON2**, catalyzed by the artificial ribonucleases **ON1x-Hg** and **ON1y-Hg$_2$**.

[28] reveals a prominent proximity effect – the former is an order of magnitude greater than the latter at the highest catalyst concentration attainable (7.0 mM) despite the fact that the latter was obtained at a much higher temperature. As expected, the local concentration of the arylmercury complex in the vicinity of the scissile phosphodiester linkage is greatly increased on tethering it to a complementary oligonucleotide. Given the similar structure of the catalytic moiety, the mechanism discussed previously [28] with arylmercury complexes as RNA cleaving agents appears likely also in the present case. Accordingly, a Hg(II) hydroxo ligand would first deprotonate the attacking 2′-OH in a rapid preequilibrium step and the resulting aqua ligand would then serve as a general acid, protonating the departing 5′-O concerted with rate-limiting rupture of the P—O5′ bond. The additional Hg(II) ion of **ON1y-Hg$_2$** does not offer any catalytic advantage, suggesting that it is oriented away from the site of reaction. The observed rate constant is, in fact, significantly smaller than the one observed with **ON1x-Hg**. Presumably the shorter and more rigid linker in **ON1y-Hg$_2$** does not allow optimal interaction of the catalytic moiety with the scissile phosphodiester linkage.

3. Conclusion

The feasibility of organometallic oligonucleotide conjugates as artificial ribonucleases has been demonstrated. Two conjugates were tested, both clearly outperforming their unmetallated counterparts as well as the parent small molecule cleaving agent in catalytic efficiency. Obviously, the activity still falls far short of the state-of-the art but the sensitivity to the length and rigidity of the linker suggests that considerable improvement through structural optimization is attainable.

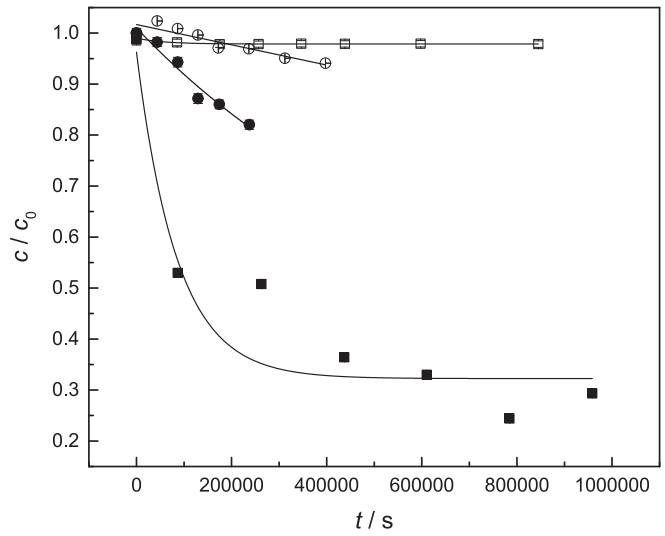

Fig. 1. Time-dependent concentration of oligonucleotide **ON2** in the presence of complementary oligonucleotides **ON1x** (□), **ON1x-Hg** (■), **ON1y** (○), **ON1y-Hg$_2$** (●); [oligonucleotides] = 0.20 μM; T = 55 °C; pH = 7.4 (20 mM cacodylate buffer); I($NaClO_4$) = 0.10 M.

4. Experimental section

4.1. General methods

The preparation of 2-(phthaliminooxy)ethyl-2-cyanoethyl-*N*,*N*-diisopropylphosphoramidite) [29,30] and 3,5-bis(acetoxymercuri)-4-hydroxybenzaldehyde [31] have been described previously. All other reagents and solvents were obtained from commercial suppliers and used as received. Solvents were dried over 4 Å molecular sieves and triethylamine over calcium hydride. The pyridine used in the preparation of oligonucleotides **ON1y** and **ON1y-Hg$_2$** and the triethylamine used in the preparation of RP-HPLC elution buffers were freshly distilled. NMR spectra were recorded on a Bruker Biospin 500 MHz NMR spectrometer. ^{1}H and ^{13}C chemical shifts (δ, ppm) were reported relative to the residual solvent peak as an internal standard and ^{31}P chemical shifts relative to external phosphoric acid. Mass spectra were recorded on a Waters Acquity RDa mass spectrometer.

4.2. 2-(2-(2-Hydroxyethoxy)ethoxy)ethyl 4-methylbenzenesulfonate (2)

Triethylene glycol (3.75 g, 25.0 mmol) was dissolved in dry dichloromethane (50 mL). The solution was cooled on an ice—water bath and silver oxide (8.69 g, 37.5 mmol) and sodium iodide (3.98 g, 26.6 mmol) were added. Finally, 4-toluenesulfonyl chloride (5.00 g, 26.3 mmol) was added portionwise over 20 min. The ice—water bath was removed and the reaction mixture was stirred for 10 min at room temperature. The mixture was filtered and the filtrate washed with 10% aqueous solution of sodium bicarbonate (50 mL). The organic phase was dried over sodium sulfate, filtered and evaporated to dryness.

Table 2
Kinetic parameters for the cleavage of the target oligonucleotide **ON2** in the presence of the complementary oligonucleotides **ON1x**, **ON1x-Hg**, **ON1y** and **ON1y-Hg$_2$**; T = 55 °C; pH = 7.4 (20 mM cacodylate buffer); I($NaClO_4$) = 0.10 M.

	k_{obs} / 10^{-6} s^{-1}	c_0	c_{eq}
ON1x	n.a.[a]	n.a.[a]	n.a.[a]
ON1x-Hg	12 ± 4	1.0 ± 0.1	0.32 ± 0.04
ON1y	n.a.[a]	n.a.[a]	n.a.[a]
ON1y-Hg$_2$	2 ± 3	1.01 ± 0.02	0.4 ± 0.9

[a] Could not be determined reliably owing to insufficient progress of the reaction.

Compound **2** was obtained as a colorless liquid in 94% yield (7.11 g). ^{1}H NMR (500 MHz, $CDCl_3$) δ: 7.67 (d, J = 8.2 Hz, 2H, Ar-H3 & H5), 7.24 (d, J = 8.0 Hz, 2H, Ar-H2 & H6), 4.05 (t, J = 4.7 Hz, 2H, CH_2OTs), 3.60—3.54 (m, 4H, 2 × CH_2), 3.50—3.41 (m, 6H, 3 × CH_2), 3.03 (d, 1H, OH), 2.33 (s, 3H, Ar-CH_3). ^{13}C NMR (126 MHz, $CDCl_3$) δ: 144.9 (Ar-C1), 132.8 (Ar-C4), 129.8 (Ar-C3 & C5), 127.8 (Ar-C2 & C6), 72.5 (CH_2), 70.5 (CH_2), 70.1 (CH_2), 69.3 (CH_2), 68.5 (CH_2), 61.4 (CH_2OH), 21.5 (Ar-CH_3). HRMS (ESI): m/z [M + Na]$^+$ calcd for $C_{13}H_{20}O_6SNa^+$ 327.0878, found 327.0876.

4.3. 2-(2-(2-(2,4-Dimethylphenoxy)ethoxy)ethoxy)ethan-1-ol (3)

2,4-Dimethylphenol (0.400 g, 3.29 mmol) and potassium carbonate (0.900 g, 6.57 mmol) were dissolved in dry *N*,*N*-dimethylformamide (5.0 mL) and the resulting mixture was stirred for 5 min at 80 °C. Compound **2** (1.00 g, 3.29 mmol) in dry *N*,*N*-dimethylformamide (1.0 mL) was added dropwise over 10 min and the reaction mixture was refluxed overnight. The solution was allowed to cool down to room temperature. After addition of cold water the mixture was extracted with dichloromethane, dried over sodium sulfate, filtered and concentrated under reduced pressure. The product was purified by silica gel column chromatography eluting with a mixture of ethyl acetate and methanol (9:1, *v*/*v*). Compound **3** was obtained as a dark yellow liquid in 47% yield (396 mg). ^{1}H NMR (500 MHz, CD_3OD) δ: 6.97—6.91 (m, 2H, Ar-H3 & H5), 6.72 (d, J = 8.1 Hz, 1H, Ar-H6), 4.09 (m, 2H, ArOCH_2), 3.86 (m, 2H, CH_2), 3.76—3.71 (m, 4H, 2 × CH_2), 3.67 (m, 2H, CH_2), 3.60 (m, 2H, CH_2), 2.27 (s, 3H, Ar-CH_3), 2.24 (s, 3H, Ar-CH_3). ^{13}C NMR (126 MHz, CD_3OD) δ: 154.8 (Ar-C1), 131.5 (Ar-C3), 129.7 (Ar-C4), 127.0 (Ar-C2), 126.6 (Ar-C5), 111.4 (Ar-C6), 72.7 (CH_2), 70.9 (CH_2), 70.4 (CH_2), 69.9 (ArOCH_2CH_2), 67.9 (ArOCH_2), 61.6 (CH_2OH), 20.4 (Ar-CH_3), 16.2 (Ar-CH_3). HRMS (ESI): m/z [M + K]$^+$ calcd for $C_{14}H_{22}O_4K^+$ 293.1155, found 293.1168.

4.4. 2-Cyanoethyl (2-(2-(2-(2,4-dimethylphenoxy)ethoxy)ethoxy)ethyl) diisopropylphosphoramidite (1)

Compound **3** (0.300 g, 1.18 mmol) was dissolved in dry dichloromethane under nitrogen atmosphere. Dry triethylamine (822 μL, 5.90 mmol) and 2-cyanoethyl-*N*,*N*-diisopropylchlorophosphoramidite (316 μL, 1.42 mmol) were added to the reaction solution. The course of the phosphitylation was followed by ^{31}P NMR spectroscopy (202 MHz, $CDCl_3$, δ = 148.9 for the product). The mixture was stirred at room temperature for 2 h and passed through a short silica gel column eluting with a mixture of triethylamine, hexane and ethyl acetate (1:66:33, *v*/*v*). Compound **1** was obtained as an oil in 96% yield (0.51 g). ^{1}H NMR (500 MHz $CDCl_3$) δ: 7.00—6.93 (m, 2H, Ar-H3 & H5), 6.74 (d, J = 8.1 Hz, 1H, Ar-H6), 4.12 (m, 2H, ArOCH_2), 3.89—3.83 (m, 4H, 2 × CH_2), 3.77—3.68 (m, 8H, $POCH_2$, 3 × CH_2), 3.63 (m, 2H, *i*Pr-CH), 2.65 (m, 2H, CH_2CN), 2.28 (s, 3H, Ar-CH_3), 2.22 (s, 3H, Ar-CH_3) 1.22—1.19 (m, 12H, *i*Pr-CH_3). ^{13}C NMR (125 MHz, $CDCl_3$) δ: 154.9 (Ar-C1), 131.5 (Ar-C3), 129.8 (Ar-C4), 126.9 (Ar-C2), 126.8 (Ar-C5), 117.7 (CN), 111.5 (Ar-C6), 70.7 (CH_2), 71.0 (CH_2), 71.2 (CH_2), 71.3 (CH_2), 70.0 (CH_2), 68.0 (CH_2), 62.6 (d, J = 17.1 Hz, $POCH_2$), 58.5 (d, J = 18.6 Hz, $POCH_2$), 43.1 (d, J = 12.6 Hz, *i*Pr-CH), 24.7 (*i*Pr-CH_3), 24.6 (*i*Pr-CH_3), 24.5 (*i*Pr-CH_3), 20.4 (Ar-CH_3), 20.3 (d, J = 6.4 Hz, CH_2CN), 16.2 (Ar-CH_3). ^{31}P NMR (202 MHz, $CDCl_3$) δ: 148.9. HRMS (ESI): m/z [M + Na]$^+$ calcd for $C_{23}H_{39}N_2O_5PNa^+$ 477.2494, found 477.2496.

4.5. Oligonucleotide synthesis

All oligonucleotides were synthesized on CPG support by an ÄKTA Oligopilot Plus 10 DNA/RNA synthesizer following standard phosphoramidite strategy with 5-(benzylthio)-1H-tetrazole as the activator. Recycle times were 120 s for **1** and the commercial 2′-*O*-methyl-RNA building blocks, 600 s for 2-(phthaliminooxy)ethyl-2-cyanoethyl-*N*,*N*-diisopropylphosphoramidite and 1200 s for the commercial TBDMS-

protected RNA building block. The phthaloyl protection of **ON1y** was removed on support by treatment with a mixture of hydrazine hydrate (35 μL), pyridine (1116 μL) and acetic acid (233 μL) for 45 min at room temperature. The support-bound aminooxy-functionalized oligonucleotide thus obtained was washed with pyridine and treated with a solution of either 4-hydroxybenzaldehyde (60 mg, 0.49 mmol) or 3,5-bis(acetoxymercuri)-4-hydroxybenzaldehyde (120 mg, 0.19 mmol) in pyridine (1.0 mL) for 2 h at room temperature. Finally, the support-bound oligonucleotide was washed with pyridine and acetonitrile and residual solvents were evaporated under vacuum. On completion of chain assembly, the oligonucleotides were released from the solid supports and the base and phosphate protections removed by overnight treatment with 25% aqueous ammonia at room temperature.

Crude **ON1x** was purified by RP-HPLC (Fig. S8 in the Supporting Information) on a SunFire C18 column (250 × 10 mm, 5 μm) eluting with a linear gradient (5—30% over 30 min) of acetonitrile in 50 mM aqueous triethylammonium acetate (pH = 7.0). The flow rate was 3.0 mL min^{-1} and the detection wavelength 260 nm. A fraction of pure **ON1x** (54.1 nmol) and mercuric acetate (541 nmol) were incubated in water (105 μL) for 22 h at 55 °C. A solution of EDTA (17 mM) in aqueous TRIS buffer (0.17 M, pH = 7.6) was added and the resulting crude product mixture purified on RP-HPLC (Fig. S10 in the Supporting Information) under otherwise the same conditions but with a steeper acetonitrile gradient (5—40% over 25 min) to afford **ON1x-Hg** in purity that was deemed satisfactory for the kinetic studies. **ON1y** and **ON1y-Hg_2** were also purified under otherwise the same conditions except that a slightly less steep acetonitrile gradient (5—40% over 30 min) was used (Figs. S12 and S14 in the Supporting Information).

The single TBDMS protection of **ON2** was removed by treatment with a mixture of triethylamine trihydrofluoride (125 μL) and DMSO (100 μL) for 150 min at 65 °C. The solution was then cooled to −20 °C and 3 M aqueous sodium acetate (25 μL) was added. The solution was shaken vigorously for 30 s, butanol (1.0 mL) was added and shaking was continued for another 30 s. The mixture was kept at −20 °C for 60 min and centrifuged. The supernatant was removed and the precipitate washed with ethanol (2 × 750 μL). The crude **ON2** thus obtained was dissolved in water and purified by RP-HPLC (Fig. S16 in the Supporting Information) on a SunFire C18 column (250 × 10 mm, 5 μm) eluting with a linear gradient (5—40% over 30 min) of acetonitrile in 50 mM aqueous triethylammonium acetate (pH = 7.0). The flow rate was 3.0 mL min^{-1} and the detection wavelength 260 nm.

The purity and identity of all of the oligonucleotide products was established by RP-UPLC-ESI-TOF-MS analysis (Fig. S9, S11, S13, S15 and S17 in the Supporting Information) on an ACQUITY Premier OST column (50 × 2.1 mm, 1.7 μm) eluting with a linear gradient (5—25% over 4 min) of methanol in an aqueous solution of hexafluoroisopropanol (40 mM) and triethylamine (7 mM). The flow rate was 0.4 mL min^{-1}, the column temperature 60 °C and the detection wavelength 254 nm. Concentrations of the oligonucleotide stock solutions were determined spectrophotometrically using molar absorptivities calculated by an implementation of the nearest-neighbors method. Contribution of the non-nucleosidic residues to the molar absorptivity was assumed to be negligible.

4.6. UV melting studies

Equimolar (1.0 μM) mixtures of the artificial ribonuclease oligonucleotides **ON1x**, **ON1x-Hg**, **ON1y** and **ON1y-Hg_2** and the target oligonucleotide **ON2** were prepared in quartz cuvettes with optical path length of 10 mm. The appropriate stock solutions were diluted to the desired concentration with 20 mM cacodylate buffer (pH = 7.4), the ionic strength of which was adjusted to 0.10 M with sodium perchlorate. UV melting profiles were measured by a PerkinElmer Lambda 35 UV/vis spectrophotometer equipped with a Peltier temperature control unit. Each measurement consisted of three heating and cooling ramps (10—90 °C, 0.5 °C min^{-1}) and absorbance at 260 nm was recorded at 0.5 °C intervals. The melting temperatures of all duplexes were too high (approximately 90 °C) to be determined accurately.

4.7. Kinetic studies

The reactions were carried out in sealed tubes thermostated at 55.0 ± 0.1 °C. The oligonucleotide (both the target and the artificial ribonuclease) concentration was 0.20 μM, the pH was adjusted to 7.4 with 20 mM cacodylate buffer and the ionic strength to 0.10 M with sodium perchlorate. The aliquots (70 μL) withdrawn from the reaction solutions at appropriate time intervals were cooled in an ice/water bath and an excess (20 equivalents) of 2-mercaptoethanol was added to effectively quench the reactions. Composition of the samples was determined by IE-HPLC on a Thermo Scientific DNASwift SAX-1S column (150 × 5 mm, monolithic). In most cases, a linear gradient (10—45% over 20 min) of 0.33 M sodium perchlorate in 20 mM aqueous triethanolamine buffer (pH = 7.0) was employed. The reaction mixture of **ON1-Hg** and **ON2** proved particularly difficult to resolve and a more denaturing solvent system, namely linear gradient (15—55% over 15 min) of 0.33 M sodium perchlorate in 20 mM aqueous triethylamine buffer (pH = 10.0) was used in this case. The flow rate was 1.5 mL min^{-1} and the detection wavelength 260 nm in all cases. The products were identified by RP-UPLC-ESI-TOF-MS analysis as described above in the context of oligonucleotide synthesis.

The chromatograms (Figs. S22—S25 in the Supporting Information) were integrated by fitting of Gaussian peaks corresponding to the starting material, the artificial ribonuclease and the products. This task was complicated by the fact that, despite extensive efforts, double helices could not be completely denatured under conditions prevailing in the IE-HPLC column, leading to broad and in some cases multiple peaks. The peak areas obtained were normalized against the total peak area and those for the target oligonucleotide **ON2** plotted as a function of reaction time. Rate constants were obtained by non-linear least-squares fitting of the first-order rate law (Eq. (1)) to these data.

CRediT authorship contribution statement

Lange Yakubu Saleh: Data curation, Investigation, Validation, Writing – original draft, Writing – review & editing. **Mikko Ora:** Supervision, Writing – review & editing. **Tuomas Lönnberg:** Conceptualization, Formal analysis, Methodology, Project administration, Resources, Supervision, Visualization, Writing – review & editing.

Declaration of Competing Interest

The authors have no competing interests to declare.

Data availability

Data will be made available on request.

Acknowledgements

Lange Yakubu Saleh gratefully acknowledges financial support from Turku University Foundation (decisions 080836 and 081007), Otto A. Malm Foundation and University of Turku Graduate School.

Appendix A. Supplementary data

Supplementary data to this article can be found online at https://doi.org/10.1016/j.jinorgbio.2023.112331.

References

[1] Y. Staroseletz, S. Gaponova, O. Patutina, E. Bichenkova, B. Amirloo, T. Heyman, D. Chiglintseva, M. Zenkova, Molecules 26 (2021) 1732.

[2] A. Kuzuya, M. Komiyama, Curr. Org. Chem. 11 (2007) 1450–1459.
[3] L. Koroleva, I. Serpokrylova, V. Vlassov, V. Silnikov, Protein Pept. Lett. 14 (2007) 151–163.
[4] A. Ghidini, M. Murtola, R. Strömberg, DNA Supramol. Chem. Nanotechnol. (2015) 158–171.
[5] F. Halloy, A. Biscans, K.E. Bujold, A. Debacker, A.C. Hill, A. Lacroix, O. Luige, R. Strömberg, L. Sundstrom, J. Vogel, A. Ghidini, RNA Biol. 19 (2022) 313–332.
[6] M. Gagliardi, A.T. Ashizawa, Biomedicines 9 (2021) 433.
[7] K.E. Lundin, O. Gissberg, C.I.E. Smith, R. Zain, Oligonucleotide-Based Ther. Methods Protoc. 2036 (2019) 3–16.
[8] X. Shen, D.R. Corey, Nucleic Acids Res. 46 (2018) 1584–1600.
[9] O.A. Patutina, S.K. Miroshnichenko, N.L. Mironova, A.V. Sen'kova, E. V. Bichenkova, D.J. Clarke, V.V. Vlassov, M.A. Zenkova, Front. Pharmacol. 10 (2019) 879.
[10] C. Gnaccarini, S. Peter, U. Scheffer, S. Vonhoff, S. Klussmann, M.W. Göbel, J. Am. Chem. Soc. 128 (2006) 8063–8067.
[11] F. Danneberg, A. Ghidini, P. Dogandzhiyski, E. Kalden, R. Strömberg, M.W. Göbel, Beilstein J. Org. Chem. 11 (2015) 493–498.
[12] P. Dogandzhiyski, A. Ghidini, F. Danneberg, R. Strömberg, M.W. Göbel, Bioconjug. Chem. 26 (2015) 2514–2519.
[13] F. Zellmann, L. Thomas, U. Scheffer, R.K. Hartmann, M.W. Göbel, Molecules 24 (2019) 807.
[14] R. Salvio, R. Cacciapaglia, L. Mandolini, F. Sansone, A. Casnati, RSC Adv. 4 (2014) 34412–34416.
[15] D. Lisi, C.A. Vezzoni, A. Casnati, F. Sansone, R. Salvio, Chem. Eur. J. 29 (2023), e202203213.
[16] N.G. Beloglazova, M.M. Fabani, N.N. Polushin, V.V. Sil'nikov, V.V. Vlassov, E. V. Bichenkova, M.A. Zenkova, J. Nucleic Acids 2011 (2011).
[17] A. Williams, Y. Staroseletz, M.A. Zenkova, L. Jeannin, H. Aojula, E.V. Bichenkova, Bioconjug. Chem. 26 (2015) 1129–1143.
[18] O.A. Patutina, E.V. Bichenkova, S.K. Miroshnichenko, N.L. Mironova, L. T. Trivoluzzi, K.K. Burusco, R.A. Bryce, V.V. Vlassov, M.A. Zenkova, Biomaterials 122 (2017) 163–178.
[19] O.A. Patutina, M.A. Bazhenov, S.K. Miroshnichenko, N.L. Mironova, D.V. Pyshnyi, V.V. Vlassov, M.A. Zenkova, Sci. Rep. 8 (2018) 1–15.
[20] M. Murtola, M. Wenska, R. Strömberg, J. Am. Chem. Soc. 132 (2010) 8984–8990.
[21] M. Murtola, A. Ghidini, P. Virta, R. Strömberg, Molecules 22 (2017) 1856.
[22] D. Desbouis, I.P. Troitsky, M.J. Belousoff, L. Spiccia, B. Graham, Coord. Chem. Rev. 256 (2012) 897–937.
[23] J. Suh, Comprehensive Inorganic Chemistry II – From Elements to Applications, Elsevier, Amsterdam, 2013, pp. 779–803.
[24] J.R. Morrow, O. Iranzo, Curr. Opin. Chem. Biol. 8 (2004) 192–200.
[25] M. Diez-Castellnou, G. Salassa, F. Mancin, P. Scrimin, Front. Chem. 7 (2019) 469.
[26] O. Luige, K. Karalė, P.P. Bose, M. Bollmark, U. Tedebark, M. Murtola, R. Strömberg, RSC Adv. 12 (2022) 5398–5406.
[27] O. Luige, P.P. Bose, R. Stulz, P. Steunenberg, O. Brun, S. Andersson, M. Murtola, R. Strömberg, Chem. Commun. 57 (2021) 10911–10914.
[28] L.Y. Saleh, M. Ora, T. Lönnberg, ChemBioChem 22 (2021) 1761–1764.
[29] T. Lönnberg, Y. Suzuki, M. Komiyama, Org. Biomol. Chem. 6 (2008) 3580–3587.
[30] Y. Xu, Y. Suzuki, T. Lönnberg, M. Komiyama, J. Am. Chem. Soc. 131 (2009) 2871–2874.
[31] T.A. Henry, T.M. Sharp, J. Chem. Soc. Trans. 121 (1922) 1055–1060.
[32] S.K. Maity, T.A. Lönnberg, ACS Omega 4 (2019) 18803–18808.
[33] L.A. Jenkins, J.K. Bashkin, M.E. Autry, J. Am. Chem. Soc. 118 (1996) 6822–6825.